Statics and Dynamics of Single DNA Molecules Confined in Nanochannels

Walter Reisner,[1] Keith J. Morton,[2] Robert Riehn,[1] Yan Mei Wang,[1] Zhaoning Yu,[2] Michael Rosen,[3] James C. Sturm,[2] Stephen Y. Chou,[2] Erwin Frey,[4] and Robert H. Austin[1,*]

[1]*Physics Department, Princeton University, Princeton, New Jersey 08544, USA*
[2]*Department of Electrical Engineering, Princeton University, Princeton, New Jersey 08544, USA*
[3]*Physics Department, Stanford University, Stanford, California 94309, USA*
[4]*Arnold Sommerfeld Center, Physics Department, Ludwig-Maximilians-Universität München, Theresienstraße 37, D-80333 München, Germany*

(Received 15 November 2004; published 16 May 2005)

The successful design of nanofluidic devices for the manipulation of biopolymers requires an understanding of how the predictions of soft condensed matter physics scale with device dimensions. Here we present measurements of DNA extended in nanochannels and show that below a critical width roughly twice the persistence length there is a crossover in the polymer physics.

DOI: 10.1103/PhysRevLett.94.196101 PACS numbers: 81.16.Nd, 82.35.Lr, 82.39.Pj

Top-down approaches to nanotechnology have the potential to revolutionize biology by making possible the construction of chip-based devices that can not only detect and separate single DNA molecules by size [1–4] but also—it is hoped in the future—actually sequence at the single molecule level [5]. While a number of top-down approaches have been proposed, all these approaches have in common the confinement of DNA to nanometer scales, typically 5–200 nm. Confinement alters the statistical mechanical properties of DNA. A DNA molecule in a nanochannel will extend along the channel axis to a substantial fraction of its full contour length [1,6]. Moreover, confinement is expected to alter the Brownian dynamics of the confined molecule [1]. While the study of confined DNA is interesting from a physics perspective, it is also critical for device design, potentially leading to new applications of nanoconfinement (for example, the use of nanochannels to prestretch and stabilize DNA before threading through a nanopore [5]). Moreover, available models [7–11] and simulations [12,13] are unable to account for the effect of varying confinement over the entire range of scales used in nanodevices. The theory gives asymptotic results valid only in limits that are not necessarily compatible with device requirements [1].

Consider a DNA molecule of contour length L, width w, and persistence length P confined to a nanochannel of width D with D less than the radius of gyration of the molecule. When $D \gg P$, the molecule is free to coil in the nanochannel and the elongation is due entirely to excluded volume interactions between segments of the polymer greatly separated in position along the backbone (see Fig. 1). de Gennes developed a scaling argument for the average extension of a confined self-avoiding polymer [8,12] which was later generalized by Schaefer and Pincus to the case of a persistent self-avoiding polymer [14]. The de Gennes theory predicts an extension r that scales with D in the following way:

$$r \cong L\left(\frac{wP}{D^2}\right)^{1/3}. \quad (1)$$

If the aspect ratio of the channel is not unity, i.e., the width $D \equiv D_1$ does not equal the depth D_2, then Eq. (1) is still valid provided that D is replaced by the geometric average of the dimensions $D_{\mathrm{av}} = \sqrt{D_1 D_2}$ [15].

As the channel width drops below the persistence length, the physics is dominated not by excluded volume but by the interplay of confinement and intrinsic DNA elasticity. In the strong confinement limit $D \ll P$, backfolding is energetically unfavorable and contour length is stored exclusively in deflections made by the polymer with the walls. These deflections occur on average over the Odijk scale $\lambda \cong (D^2 P)^{1/3}$ [7,13]. The extension is the number of Odijk segments $\frac{L}{\lambda}$ times the average projection of an Odijk segment on the channel axis. Assuming that the average deflection made by the polymer with the walls is small, $\cos(\theta) \approx 1 - \frac{1}{2}\theta^2$, $\theta \approx \frac{D}{\lambda}$ and

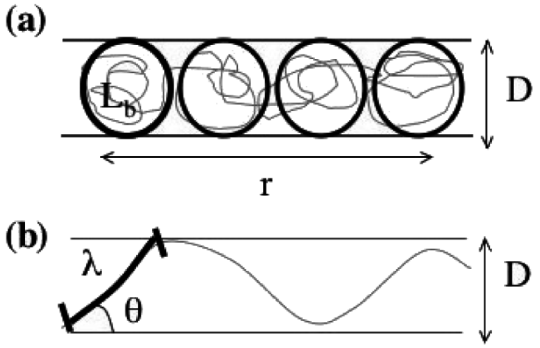

FIG. 1. (a) A confined polymer in the de Gennes regime: $D \gg P$. The molecule can be subdivided equally into a series of blobs with contour length L_b; the stretch arises from the mutual repulsion of the blobs. (b) A confined polymer in the Odijk regime: $D \ll P$.

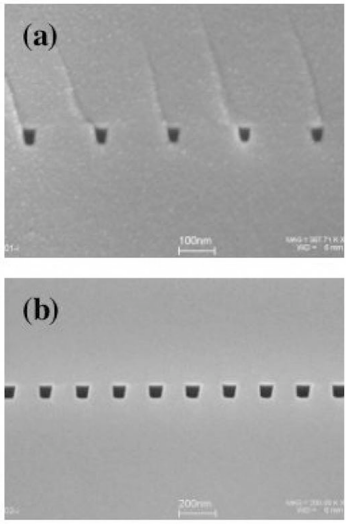

FIG. 2. (a) Cross-sectional scanning electron micrographs of 30×40 nm nanoimprinted channels and (b) 60×80 nm nanoimprinted channels. The channels are shown sealed to a fused silica coverslip (the sealing was accomplished via direct quartz-quartz bonding). Imprinted nanochannels are densely packed with a periodicity of 200 nm and width that can be varied from 150 to 35 nm using a novel trilayer technique (wider channels can also be fabricated with a correspondingly higher period) [18].

$$r = L\cos(\theta) = L\left[1 - A\left(\frac{D}{P}\right)^{2/3}\right]. \quad (2)$$

Reference [7] finds that $A \cong 0.361$. In the Odijk regime, D can not be rigorously replaced by D_{av} if the channel aspect ratio is not unity. In the case that D_1 and D_2 are close then the substitution is a reasonable approximation. The nature of the crossover behavior between the de Gennes and Odijk regimes, $D \sim P$, is not currently understood. The crossover regime is important as it is likely to occur within the range of scales used in devices: the persistence length of double stranded DNA (dsDNA) is roughly 50 nm in standard electrophoresis buffers [16].

The nanochannels used in this study were nanofabricated on fused silica substrates using a combination of two techniques: (1) nanoimprint lithography [17,18] and (2) electron beam lithography using a Leica/Cambridge EBMF system at the Cornell Nanofabrication Facility (CNF). Figure 2 shows images of sealed channels. Additional details concerning chip fabrication can be found in [1].

The sealed devices were wet with a loading buffer consisting of 0.045 M tris-base, 1 mM EDTA with 0.045 M boric acid ($0.5 \times$ TBE). To suppress bleaching and photonicking of confined DNA, an oxygen scavenging system was added consisting of 4 mg/ml $\beta - D$ glucose, 0.2 mg/ml glucose oxidase, 0.04 mg/ml catalase and 0.07 M β-mercaptoethanol. The oxygen scavenging system suppressed from nicking for around 2 hours, after which a buffer with a fresh O_2 system was added. The DNA was dyed with TOTO-1 fluorescent dye (Molecular Probes) at a concentration of 1 dye molecule per every 10 base pairs. Previous experiments investigating the stretching of DNA stained with intercalating dyes suggest that the dye, to first approximation, just increases the contour length and persistence length up to a saturating value of 30% [19–21]. The saturating dye concentration is 1 dye molecule per 4 base pairs, so at our dye concentration (40% of full dying) we expect an increase of 13%, yielding a

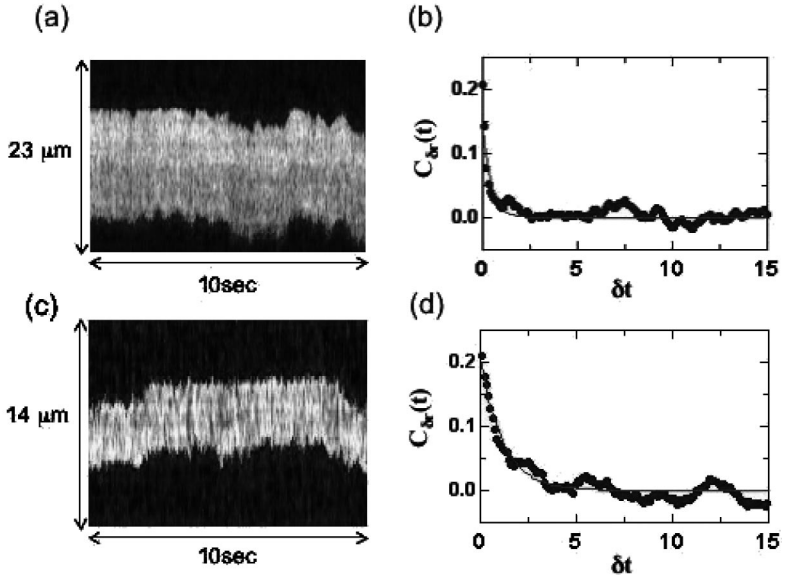

FIG. 3. (a) Time evolution of intensity stripe for a λ-phage DNA molecule in a 60 nm channel. (b) Autocorrelated extension fluctuation extracted from the molecule shown in (a) with exponential fit. (c) Time evolution of intensity stripe for a λ-phage DNA molecule in a 180 nm channel. (d) Autocorrelated extension fluctuation for the molecule shown in (c) with exponential fit. The black dots at the stripe edges in figures (a) and (c) represent the edges of the molecules determined via an edge-finding algorithm.

contour length of 18.6 μm and a persistence length of 57.5 $\pm$ 2 nm (using the value for the persistence length obtained in [16]). Experiments were conducted either with λ-phage DNA (48.5 kbp, $L = 16.5$ μm, $L_{\text{dye}} = 18.6$ μm, New England Biosciences) or T2 DNA (164 kbp, $L = 55.8$ μm, $L_{\text{dye}} = 63$ μm, Sigma). The DNA molecules were driven electrophoretically into the nanochannels. Their fluctuations were then recorded with a Pentamax ICCD camera (Roper Scientific) on a Nikon Eclipse TE300 microscope using a 100$\times$ N.A.1.4 oil immersion objective (Nikon). Typically, a group of molecules was imaged for 500–2500 frames at a time.

For a given molecule the intensity transverse to the channel axis was summed to obtain a 1D intensity scan $I(z)$ along the channel axis. The intensity scan was assumed to be a convolution of a step function I_o of length r with a Gaussian point spread function yielding the erf model fitting function discussed in [1]. The extension was extracted from each frame using the fitting function and the resulting extension fluctuations δr about the mean extension r were used to obtain the autocorrelation function $C_{\delta r} = <\delta r(t)\delta r(t + \delta t)>$. Exponential fits to $C_{\delta r}$ yield the relaxation time (see Fig. 3). The extension and relaxation time were then averaged over as many molecules as could be conveniently measured in a single experiment to obtain the best estimates of r and τ for a given channel width and molecule size (typically, 10–30 molecules were used).

Figure 4 shows images of λ-phage and T2 dsDNA molecules confined in the nanochannels. The stretching of the polymers is clearly a function of the channel width and plateaus as the width drops below the persistence length. Figure 5 shows a plot of the DNA extension versus the geometric average of the nanochannel dimensions. The data fits well to a power law with the clear exception of the data point for the 30 nm channel, suggesting that the smallest channel is in the Odijk regime. The transition scale can be precisely defined by requiring that Eq. (2) and the power-law fit merge continuously at a critical scale D_{critical}. This stipulation enforces $D_{\text{critical}} = \gamma P$, with the proportionality constant $\gamma = 1.93$ fixed entirely by the power-law exponent and the value of A in Eq. (2).

Further confirmation of the crossover scale arises from examination of the measured relaxation times as a function of D_{av}, shown in Fig. 6. This data shows that the relaxation times are maximized between 80 and 130 nm, consistent with $D_{\text{critical}} = 1.9P = 110$ nm. To explain the existence of this maximum, note that the relaxation time scales as the ratio of a friction factor ξ to an effective spring constant k (for small displacements about the equilibrium extension). The self-avoidance model predicts a friction factor that increases slightly faster than the spring constant, leading to a relaxation time that increases slowly with decreasing width [1,9]. The situation is reversed in the Odijk regime: for $D \ll P$ the relaxation time rapidly decreases with decreasing width due to the strong scaling of the spring constant with width in this regime.

A scaling relation for the relaxation time in the limit $D \ll P$ is straightforward to obtain using the free energy predicted by the Odijk model. The free energy is k_BT times the number of Odijk segments [7,13]:

$$\Delta F_{\text{conf}} \cong k_BT \frac{L}{(D^2P)^{1/3}}. \quad (3)$$

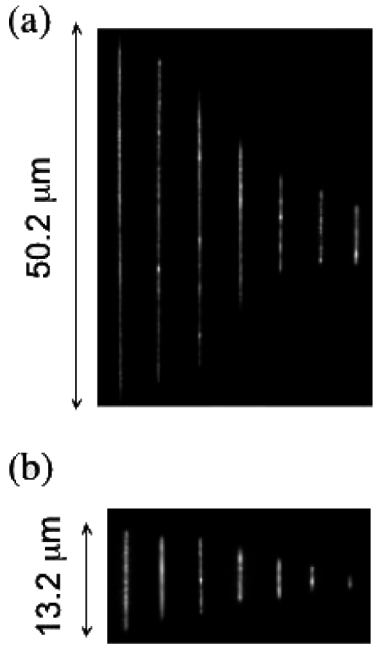

FIG. 4. (a) Averaged intensity of selected T2 DNA molecules in 30×40 nm, 60×80 nm, 80×80 nm, 140×130 nm, 230×150 nm, 300×440 nm, and 440×440 nm channels (left to right). (b) Averaged intensity of selected λ-DNA molecules in the same channels.

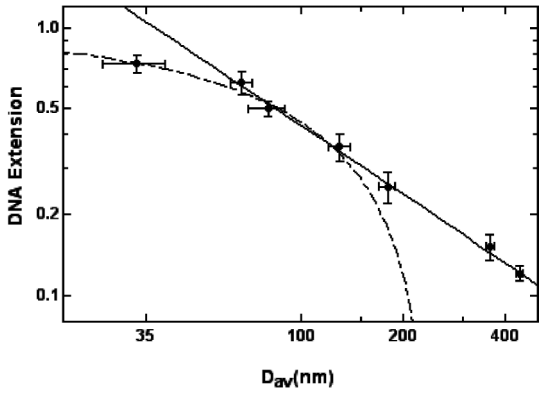

FIG. 5. Log-log plot of λ-DNA extension as a function of D_{av}, the geometric average of the channel depth and height. The DNA extension is normalized to the (dye-adjusted) total contour length of 18.63 μm. The bold line is a best power-law fit to the data for the 440, 300, 230 , 140, 80, and 60 nm wide channels (the best fit exponent is -0.85 ± 0.05). The dashed line is the Odijk prediction, which fits to the three smallest channels with a persistence length of 52 $\pm$ 5 nm, in agreement with the dye-adjusted persistence length of 57.5 $\pm$ 2 nm.

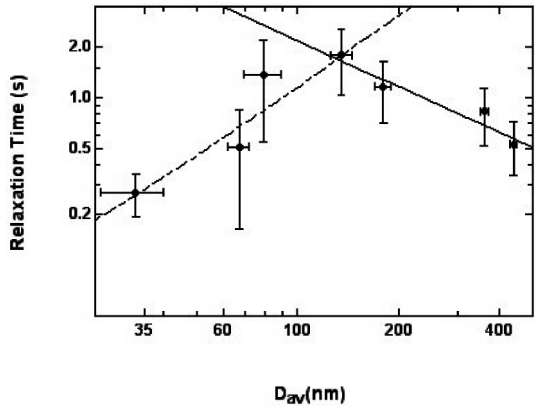

FIG. 6. Log-log plot of λ-DNA relaxation time as a function of D_{av}, the geometric average of the channel depth and height. The data points shown are averages over all the relaxation times measured for molecules in a given width. Shown superimposed is a best power-law fit to the data taken for channels greater than 140 nm (bold curve) and a fit to the model $\tau \sim \frac{D^{\alpha}}{\log(D/w)}$ for channel widths less than 140 nm (dashed curve). The de Gennes theory underestimates the scaling exponent: the best fit exponent for the large channel widths is -0.9 ± 0.4. The best fit exponent for the small widths is $\alpha = 1.6 \pm 0.4$.

By eliminating D between the equations for the extension [Eq. (2)] and the free energy [Eq. (3)], differentiating twice with respect to r, and then solving in terms of D, we obtain the spring constant:

$$k_{\mathrm{Odijk}} \cong \frac{k_B T}{L} \frac{P}{D^2}. \tag{4}$$

In the Odijk limit the friction arises entirely from the hydrodynamic interaction of a segment of DNA $\sim D$ with the channel wall. The wall-DNA interactions lead to a friction factor $\xi \cong \frac{2\pi\eta L}{\log(D/w)}$ [11,22]. Then,

$$\tau_{\mathrm{Odijk}} \cong \frac{\eta L^2}{k_B T} \frac{D^2}{P \log \frac{D}{w}}. \tag{5}$$

Physically, this time scale arises from the diffusion of contour along the tube [10]. [We note that there is a controversy in the literature over the correct scaling of the relaxation time with width [11]. Morse argues that the exponent is 2 [11], in agreement with Eq. (5), while Maggs argues that the exponent is $4/3$ [10,23].]

In conclusion, we have extracted the extensions and relaxation times for DNA molecules stretched in nanochannels with widths ranging from 30 to 400 nm. We have identified a crossover scale D_{critical} roughly twice the persistence length that determines the degree of confinement at which bending rigidity becomes significant. The behavior of the extension for widths greater than the crossover scale is consistent with a power law of the form $\sim D^{-0.85}$. This result differs from the classic de Gennes theory [8], which predicts the extension should scale as $D^{-2/3}$. We feel Monte Carlo studies of confined DNA are essential to clarify the situation.

This work was supported by grants from DARPA (MDA972-00-1-0031), NIH (HG01506), NSF Nanobiology Technology Center (BSCECS9876771), the State of New Jersey (NJCST 99-100-082-2042-007) and US Genomics. It was also performed in part at the Cornell Nano-Scale Science and Technology Facility (CNF) which is supported by the National Science Foundation under Grant No. ECS-9731293, its users, Cornell University, and Industrial Affiliates. We thank O. Hallatschek, L. Latanzi, and Frederik Wagner for illuminating discussions in Berlin. We also thank P. Silberzan and J. Tegenfeldt for numerous suggestions and discussions.

*Electronic address: austin@princeton.edu

[1] J. Tegenfeldt, C. Prinz, H. Cao, S. Chou, W. Reisner, R. Riehn, Y. M. Wang, E. C. Cox, J. C. Sturm, P. Silberzan, and R. H.Austin, Proc. Natl. Acad. Sci. U.S.A. **101**, 10979 (2004).
[2] S. W. P. Turner, M. Cabodi, and H. G. Craighead, Phys. Rev. Lett. **88**, 128103 (2002).
[3] J. Han, S. W. Turner, and H. G. Craighead, Phys. Rev. Lett. **83**, 1688 (1999).
[4] J. Li, M. Gershow, D. Stein, E. Brandin, and J. A. Golovchenko, Nat. Mater. **2**, 611 (2003).
[5] R. Austin, Nat. Mater. **2**, 567 (2003).
[6] L. J. Guo, X. Cheng, and C. F. Chou, Nano Lett. **4**, 69 (2004).
[7] T. Odijk, Macromolecules **16**, 1340 (1983).
[8] P. G. de Gennes, *Scaling Concepts in Polymer Physics* (Cornell University Press, Ithaca, NY, 1979).
[9] F. Brochard and P. G. de Gennes, J. Chem. Phys. **67**, 52 (1977).
[10] H. Isambert and A. C. Maggs, Macromolecules **29**, 1036 (1996).
[11] D. C. Morse, Macromolecules **31**, 7044 (1998).
[12] R. M. Jendrejack, D. C. Schwartz, M. D. Graham, and J. J. Pablo, J. Chem. Phys.. **119**, 1165 (2003).
[13] M. D. Dijkstra, D. Frenkel, and H. N. W. Lekkerkerker, Physica A (Amsterdam) **193**, 374 (1993).
[14] D. W. Schaefer, J. F. Joanny, and P. Pincus, Macromolecules **13**, 1280 (1980).
[15] L. Turban, J. Phys. (Paris) **45**, 347 (1984).
[16] C. Bouchiat, M. D. Wang, J. F. Allemand, T. Strick, S. M. Block, and V. Croquette, Biophys. J. **76**, 409 (1999).
[17] S. Y. Chou, P. R. Krauss, and P. J. Renstrom, Appl. Phys. Lett. **67**, 3114 (1995).
[18] Z. N. Yu, H. Gao, W. Wu, H. X. Ge, and S. Y.Chou, J. Vac. Sci. Technol. B **21**, 2874 (2003).
[19] O. B. Bakajin, T. A. J. Duke, C. F. Chou, S. S. Chan, R. H. Austin, and E. C. Cox, Phys. Rev. Lett. **80**, 2737 (1998).
[20] S. B. Smith, L. Finzi, and C. Bustamante, Science **258**, 1122 (1992).
[21] T. Perkins, D. E. Smith, R. G. Larson, and S. Chu, Science **268**, 83 (1995).
[22] G. K. Batchelor, *An Introduction to Fluid Dynamics* (Cambridge University Press, Cambridge, England, 1967).
[23] A. C. Maggs, Phys. Rev. E **55**, 7396 (1997).